

# A nanodevice for rectification and pumping ions

Zuzanna Siwy<sup>a)</sup>

GSI, Darmstadt, Planckstrasse 1, 64291 Darmstadt, Germany  
and Silesian University of Technology, 44-100 Gliwice, Poland

Andrzej Fuliński

Jagellonian University, Institute of Physics, 30-059 Kraków, Poland

(Received 11 March 2003; accepted 19 December 2003)

The transport properties of single asymmetric nanopores in polyethylene terephthalate (PET) are examined. The pores were produced by a track etching technique based on the irradiation of the foils by swift heavy ions and subsequent chemical etching. Electrical conductivity measurements show that the nanopores in PET are cation selective and rectify the current with the preferential direction of cation flow from the narrow entrance toward the wide opening of the pore. Moreover, the pore transports potassium ions against the concentration gradient if stimulated by external field fluctuations. We show that the rectifying and pumping effects are based on the ratchet mechanism.

© 2004 American Association of Physics Teachers.

[DOI: 10.1119/1.1648328]

## I. INTRODUCTION

The words of Richard Feynman, “There is plenty of room at the bottom,”<sup>1</sup> suggest that when the dimensions of objects approach the nanometer scale we might observe new properties occurring due to the restricted geometry.<sup>2</sup> Physicists are well prepared to explore the nanoworld and to follow Feynman’s suggestion to look for the laws governing it. In the 1940s transmission electron microscopy enabled researchers to obtain a resolution of 1 nm. The scanning tunneling microscope and atomic force microscope led to the possibility of seeing single atoms. There are techniques for producing nanostructures such as nanowires, nanotubes (see, for example, Refs. 3–8), and quantum dots.<sup>9,10</sup>

The biggest challenge at present is to create devices based on nanostructures (see, for example, Ref. 11). At the same time, scientists have begun to look at the various nanomachines in living organisms. As an example consider a cell with nanometer sized ion channels embedded in the cell membrane. The channels are the principal nanodevices mediating the communication of a cell with other cells via ion transport,<sup>12–14</sup> and enable the functioning of a living organism. There is a great variety of ion channels that fulfill various tasks. For example, there are channels that function as diodes for an ionic current—they have a preferential direction of ion flow and block almost completely ions moving in the other direction.<sup>12</sup> The channels called ion pumps are able to transfer ions against their concentration gradient at the expense of energy coming from the hydrolysis of ATP.<sup>15</sup> Many channels are highly selective for particular ions and can be controlled by an applied electric field, a molecule bound to the membrane, or applied mechanical stress.<sup>12</sup>

Another fascinating property of ion channels is the fluctuating ion current signal for a constant voltage across the membrane (see, for example, Refs. 16 and 17). The current usually switches between just two values: zero, representing a closed state of the channel, and a nonzero one, which is called an open state of the channel. The pattern of switching between these states is different for various channels. For voltage-gated channels it depends on the external voltage.<sup>17</sup> Although the structure of some channels is known,<sup>18–20</sup> there are still many aspects of ion transport that are not yet well

understood. The phenomenon of ion current fluctuations is one of the unsolved puzzles (see however, Ref. 21). There also are open questions regarding ion current rectification and pumping.

It has been shown that a protein nanopore (for example, the  $\alpha$ -hemolysin channel) can function as a biosensor for biomolecules, for example, DNA.<sup>22</sup> The sensing procedure is based on directing the biomolecule to the pore by means of an electric field. When passing through the pore, a biomolecule brings about its temporary blockage, which is observed as a change in the ion current signal. The ion current changes depend on the structure and chemistry of the biomolecule (for example, the DNA sequence),<sup>22</sup> which is the basis of its detection. Because many biomolecules are charged, this detection method can potentially be very widely applied and does not require any chemical pretreatment of the molecules, which is a big advantage over other detection techniques.

To design biosensors and learn about ion transport in nanochannels, it would be very helpful to have a synthetic, robust system that is much easier to understand and describe. It would also allow us to perform experimental studies not applicable to biochannels due to their fragile nature. First, however, we have to determine whether synthetic pores can function as analogs of biochannels. In other words, if we could prepare pores in a synthetic film of dimensions similar to these of biochannels, would it be possible to observe similar transport properties, for example, ion current fluctuations, rectification, and pumping?

Earlier studies performed by the groups of Lev, Pasternak, and Korchev (see, for example, Refs. 23 and 24), together with our recent experimental results,<sup>21,25,26</sup> indicate that the answers to these questions can be positive. The time series recorded for the biological and synthetic channels were found very similar. The ion current through the channels fluctuates between discrete levels, and it is very difficult to differentiate between the signals, both the original time series, and their power spectra.<sup>21</sup>

The rectification of ion currents also has been demonstrated for synthetic pores. Our recent experimental results show that an asymmetric, conically shaped nanopore in poly-

ethylene terephthalate (PET) and polyimide is cation selective and rectifies the cation flow from the narrow entrance toward the wide opening of the pore.<sup>25–27</sup>

However, we can ask further questions. Would it be possible to construct a synthetic nanopore such that when it is stimulated by external electric field fluctuations, it is able to transport ions against their concentration gradient, an effect observed for biopumps? We expected that such a system would possess an internal preferential direction of ion flow and be able to counteract the diffusion flow. Therefore, a conically shaped nanopore seemed to be a good starting point for an ion pump. Our predictions were further strengthened by the discussion in Ref. 28 of the decisive role of asymmetry in the functioning of rectifying nanodevices.<sup>28</sup> An asymmetric semiconductor quantum dot and an asymmetric biological channel rectify the current: both devices possess a preferential direction for the current flow—the first device for the electron flow and the other one for ions.<sup>28</sup> Moreover, a micrometer sized synthetic realization of asymmetric channels has been accomplished recently: fabricated asymmetric micropores were shown to rectify the transport of negatively charged latex microbeads.<sup>29</sup>

All these devices work on the ratchet principle (see, for example, Refs. 30–32), which uses the asymmetry (spatial or temporal) of the potential in which the particle moves. The ratchet potential is usually visualized as an asymmetric sawtooth (or a series of saw-teeth) like the one shown in Fig. 4(b). It represents the distribution of, for example, the electric, chemical potential, or temperature. It has been shown that nonequilibrium fluctuations can bias the Brownian motion of particles in the asymmetric potential without macroscopic forces (for example, thermal gradients, macroscopic electric field). We also know that the ratchet principle can explain the mechanism by which biological pumps (AT-Pases) function.<sup>33</sup>

These results and the idea that asymmetric nanochannels might offer a possibility of performing both rectification and pumping of ions on a nanoscale motivated us to fabricate them.

The preparation of the asymmetric nanopores by a track-etching technique is described briefly in Sec. II. Sections III and IV discuss the transport properties of the nanopores. The single pore current–voltage characteristics were measured and rectification together with the pumping effect was demonstrated. We show that the electric potential inside a conical pore has the shape of an asymmetric tooth, and the pore transports ions according to a ratchet mechanism. The calculation of the motion of an ion in the asymmetric potential inside a conical pore confirmed the existence of the preferential direction of cation flow (see Sec. V). In Sec. VI we describe the ion current by the Smoluchowski equation.

## II. A UNIQUE TOOL TO STRUCTURE MATERIALS ON A NANOMETER SCALE

To follow the properties of ion transport in nanochannels, the best system to study is a membrane with only one nanopore. We thus avoid the averaging effects coming from the ion flow through many pores as well as the problem of separating one pore out of many. We looked for a technique that makes it possible to obtain a membrane with a given number of pores. The unique tool to do this is the track etching technique.<sup>34,35</sup> This nanofabrication technique is based on the irradiation of dielectric foils with energetic heavy ions be-

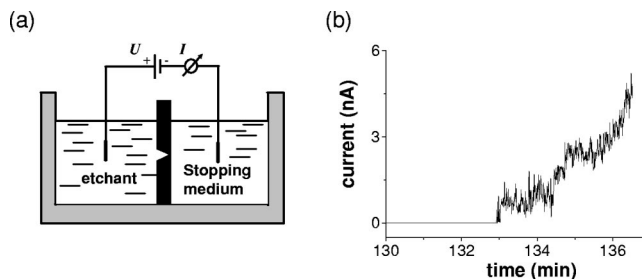


Fig. 1. (a) Conductivity cell used to prepare the single conical pores, and (b) an example of an etching curve.

tween 1 and  $10^{12}$  ions per square cm. The zone of the damaged material along the straight ion paths (commonly named latent tracks) is several nanometers in diameter and is characterized by an extremely high length/width ratio of  $10^4$ . The irradiated foils are therefore an excellent starting point for producing membranes with very small pores. The damaged track zone is selectively removed by chemical etching, leaving the pristine material almost intact. The number of pores is determined by the number of incident ions.<sup>36</sup>

By a proper choice of etchant, temperature, and etch time, the diameter of the resulting pores can be adjusted to be between  $10\ \mu\text{m}$  and  $10\ \text{nm}$ . The etching conditions also determine the shape of the pores. To obtain a conical shape, the foil is placed between two chambers of a conductivity cell and etched from one side [Fig. 1(a)]. The other chamber is filled with a stopping medium that neutralizes the etchant.<sup>25</sup> For example, if NaOH is used as an etchant, the stopping medium is acidic. The etching is controlled by monitoring the current [Fig. 1(b)]. Because the tracks left in material by energetic heavy ions are not permeable to ions, the current in the beginning of the etching process is zero. When the pore is etched through, the current increases gradually, showing unambiguously the opening of the pore as well as reflecting the increase of the pore diameter. To obtain nanopores, the etching has to be stopped shortly after the break through. For our studies we used commercially available polyethylene terephthalate (PET) foils that are  $12\ \mu\text{m}$  thick.<sup>37</sup> It is known that the cleavage of polymeric chains during irradiation and etching produces carboxylate groups. The degree of carboxylate groups deprotonation, and therefore the pore surface charge, is regulated by the electrolyte pH. At neutral pH, the carboxylate groups are dissociated and the pore is negatively charged. Lowering the pH value results in protonation of the groups and diminishing the surface charge. There is a value of pH, characteristic for a given surface and molecules (for example, proteins), called an isoelectric point, for which the net surface charge is zero. The isoelectric point for the etched PET is  $\sim 3.8$ . The issue of surface charge is very important, because when ions pass through a narrow pore, they interact with charges on the pore wall, influencing the pore transport properties.

## III. AN ASYMMETRIC PORE RECTIFIES THE ION CURRENT

After washing in distilled water the pore is ready for further measurements. We begin with determination of the current–voltage ( $I$ – $V$ ) characteristics. This measurement is done by applying a ramp, triangular, or sine wave voltage, and simultaneously recording the ion current. The important

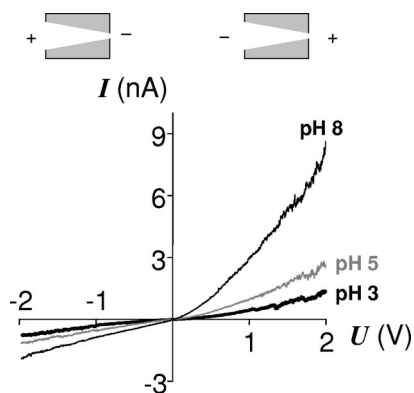


Fig. 2. The current–voltage characteristics for a single conical pore in PET recorded at symmetric electrolyte conditions on both sides of the membrane at 0.1 M KCl and various  $pH$  values. Note the sign convention for the applied potential difference.

factor is the sign of the applied potential difference (Fig. 2). We have found that the conical pores for neutral and basic  $pH$  values for which their walls are negatively charged show distinctly nonlinear  $I$ – $V$  curves. The nonlinearity becomes more pronounced at higher voltages.<sup>25</sup> The question we had to answer at the very beginning is which ions contribute to the recorded current, that is, whether the pore is cation or anion selective. Ion selectivity is usually expressed by the transference numbers of cations ( $t_+$ ) and anions ( $t_-$ ) within the membrane. The sum of transference numbers is 1, and  $t_+$  and  $t_-$  indicate the percentage of the current signal carried by cations and anions, respectively. The quantities  $t_+$  and  $t_-$  can be determined in a conductivity cell in which the membrane separates two electrolyte solutions of the same salt but of different concentrations. The resulting potential difference for 1:1 salt is given by<sup>38</sup>

$$E_m = (2.303RT/nF)(t_+ - t_-)\log(c_1/c_2), \quad (1)$$

where  $F$  is the Faraday constant equal to 96 485 C/mol, and  $n$  stands for charge of ions. For the PET membrane and ten-fold concentration gradient of KCl ( $c_1/c_2 = 10$ ),  $E_m \approx 50$  mV, which gives  $t_+ \sim 0.9$  (and  $t_- \sim 0.1$ ). That is, 90% of the current signal is therefore due to potassium ions.

If we take into account the polarity of the applied voltage, we can establish the preferential direction of the cation flow. Surprisingly, we find that the potassium ion flow is higher in the direction from the narrow entrance toward the wide opening of the pore. It contradicts our intuition about a funnel, in which we always pour a liquid through the wide opening.

We have checked the transport properties of the pores whose surface charge was neutralized by protons at  $pH$  3. Under those conditions the pore practically stopped rectifying and obeyed Ohm's law (Fig. 2). This result suggests that the asymmetry of the pore may change the electrostatic barrier for ions entering the pore.

Measurements of the  $I$ – $V$  characteristics let us estimate the size of the pores by using the relation between the pore's resistance and its geometry, the length  $L$  and cross-section  $A$ :

$$R = \frac{1}{\Lambda} \frac{L}{A}, \quad (2)$$

where  $\Lambda$  is the conductivity of the electrolyte. The value of  $R$  is found from the slope of the  $I$ – $V$  curve. The measurements have to be performed at high electrolyte concentrations and low  $pH$  values. For these conditions the conductivity of the solution inside the pore approaches the value in the bulk. The relation (2) is valid only for systems for which the length of the pores is much larger than their radius  $r$ . In our experiments the aspect ratio,  $L/r$ , always exceeds 100. When the aspect ratio is small, the distortion of the current streamlines at the pore entrance has to be taken into account as an additional resistance, known as an entry resistance. It has been shown that the length of the pore has to be replaced in Eq. (2) by the effective length  $L_{\text{eff}} = L + 1.64r$ .<sup>39</sup>

For a conical geometry, Eq. (2) becomes more complex due to the varying cross section (see Problem 1), and the final expression for the resistance of a conical pore is

$$R = \frac{1}{\pi\Lambda} \frac{L}{r_L r_0}, \quad (3)$$

where  $r_L$  and  $r_0$  denote the radii of the large and the small openings of the conical pore, respectively. Due to the large aspect ratio of the pores, the entry resistance is a very small percentage of the total resistance of the system, and we do not consider it further.

**Problem 1:** Derive Eq. (3) for the resistance of a conical pore of length  $L$  and the radii of two the openings equal to  $r_L$  and  $r_0$ , respectively. Estimate quantitatively and qualitatively the change in the pore's resistance with decreasing opening angle of the cone.

If we know the conductivity of the electrolyte, the radius of the large opening of the pore, the membrane's thickness, and assume a perfect conical geometry, we can calculate the radius of the small pore opening. At present, we can successfully prepare membranes with an effective pore radius of approximately 1 nm.

We have also checked how the rectifying properties of the pores depend on the size of the small opening of the pore. We have found that the diode-like current–voltage characteristic results from the nanometer size of the pores. When the diameter of the small opening is larger than approximately 15 nm, the resistance of the pore satisfies a linear  $I$ – $V$  relation.

#### IV. CAN THE IONS BE TRANSPORTED AGAINST A CONCENTRATION GRADIENT?

As we have shown in Sec. III, one way to change the  $I$ – $V$  characteristic of a conical pore from a nonlinear form to an ohmic one is by neutralizing the surface charge. Another way to make the pore stop rectifying could be based on counteracting the preferential direction of cation current with a diffusion flow.<sup>40</sup> If the side of the membrane with the wide pore opening is in contact with an electrolyte solution of higher concentration, the diffusion flow opposes the observed intrinsic preferential direction of the current (see Fig. 3). We measured the ion current–voltage characteristics for various concentration gradients and applied alternating voltage signals of amplitudes in the range 0–0.8 V and zero mean. Figure 3 shows the applied voltage together with the ion current, which was recorded for the concentration gradient 0.1 M/0.75 M KCl, and two amplitudes of the ac voltage signal equal to 100 and 400 mV, respectively. A negative value for the current indicates that the direction of potassium ion flow

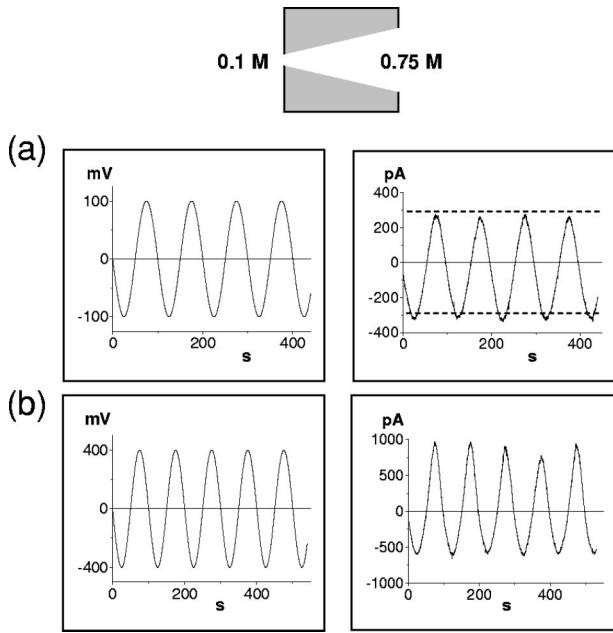


Fig. 3. Signals of the applied ac voltage vs time for two amplitudes (a) 100 mV and (b) 400 mV, together with ion current, measured simultaneously. The measurements were performed with the concentration gradient 0.1 M KCl/0.75 M KCl as shown.

is in the direction of the concentration gradient. We see that a higher amplitude for the applied voltage oscillation reverses the direction of potassium flow. The ions are then transported against the concentration gradient, and therefore they are pumped. To quantify the pumping effect of the pore, we can calculate an average current (average over the period of the ac signal), which gives the net flow.

It is remarkable that the pumping of ions by means of an oscillating electric field in the absence of ATP has also been observed for biological channels.<sup>41–45</sup> Extensive theoretical studies on the role of nonequilibrium fluctuations (“noise”) on the function of ion pumps has been performed.<sup>46–50</sup>

## V. WHY DOES THE NANOPORE RECTIFY AND PUMP THE IONS?

Before modeling the rectification and pumping observed for conical pores, we point out the properties of the system that are crucial for these effects: (i) the conical shape of the pore (on the basis of our previous experiments we know that cylindrical pores do not rectify the ion current), (ii) the nanometer size of the small opening, and (iii) the surface charge of the pores. If these three features are sufficient to explain the asymmetry of the  $I-V$  curves, it would imply that our model predicts rectification properties of any narrow enough conical pore with charges.

Figure 4 shows our model: a conical pore with a homogeneous charge distribution on the walls onto which a potassium ion is placed. We start by considering the electrostatic interactions of a potassium ion with the negative charges on the pore walls. We first recall how interactions between two charges depend on the medium in which they are placed. In vacuum, the Coulomb interaction energy between two charges separated by a distance  $r$  is given by

$$U(r) = \frac{1}{4\pi\epsilon_0} \frac{q_1 q_2}{r}. \quad (4)$$

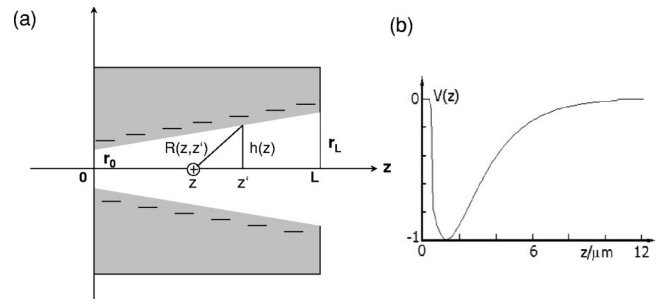


Fig. 4. (a) Schematic axial cut through a channel. For the sake of clarity, the proportions differ from a real pore. (b) The profile of potential  $V(z)$  inside an asymmetric pore calculated from Eq. (7) for  $r_0=3$  nm,  $r_L=250$  nm,  $1/\lambda=40$  nm, and  $\gamma/m=1$  s<sup>-1</sup>.

When the interactions take place in a polarizable dielectric medium, the Coulomb interactions are reduced by a dimensionless dielectric constant  $\epsilon$ :

$$U(r) = \frac{1}{4\pi\epsilon\epsilon_0} \frac{q_1 q_2}{r}. \quad (5)$$

The screening in an electrolyte solution comes not only from water ( $\epsilon=80$ ), but also from the presence of other ions in the solution. This additional weakening of the interactions is described by the Debye potential:

$$U(r) = k' \frac{q_1 q_2}{r} e^{-\lambda r}. \quad (6)$$

The parameter  $\lambda$  measures the effectiveness of the screening.

Now, we are prepared to calculate the internal electric potential  $V(z)$  on the cone axis  $z$  [see Fig. 4(a) for an explanation of the symbols]:

$$V(z) = -2\pi\rho \int_0^L dz' h(z') e^{-\lambda R(z, z')}/R(z, z'), \quad (7)$$

and write the equation of motion of an ion along the  $z$  axis driven by an oscillating periodic force  $A \sin(\Omega t)$ :

$$m \frac{d^2 z}{dt^2} + \gamma \frac{dz}{dt} = F(z) + A \sin(\Omega t), \quad (8)$$

where  $m$  is the ion mass,  $\gamma$  the friction coefficient, and  $F(z) = -\partial V(z)/\partial z$ .

*Problem 2:* In our original paper<sup>40</sup> we gave a formula for  $F(z)$  [instead of  $V(z)$ ] for a two-dimensional “cone.” (a) Find the corresponding two-dimensional formulas for  $V(z)$  and  $F(z)$ . (b) Explain how and why the two-dimensional and three-dimensional expressions differ from each other.

Figure 4(b) shows the shape of the electrostatic potential obtained from Eq. (7) for  $r_0=3$  nm,  $r_L=250$  nm,  $1/\lambda=40$  nm,  $\gamma/m=1$  s<sup>-1</sup>, and  $\rho=1$  nm<sup>-2</sup>. The potential has the shape of an asymmetric sawtooth which implies more negative potential close to the narrow entrance to the pore than at the wide pore opening. A qualitatively similar character for  $V(z)$  has been obtained for a wide range of parameters (for example, for smaller  $r_0$  and large  $\lambda$ , for which the asymmetry becomes more pronounced).

Now we can draw a qualitative picture of the rectification and pumping model. If we apply a potential difference across the membrane (therefore an additional force on the ions), we obtain a tilting of the potential tooth in one or another direc-

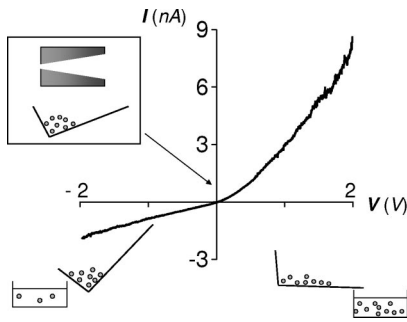


Fig. 5. Schematic representation of the principles that describe how a conical pore rectifies the ion current. The asymmetric conical pore has an internal potential in a form of an asymmetric tooth. Changing the polarity of the external potential difference changes the height of the potential barrier. The potential is “rocked” resulting in the net flow.

tion depending on the polarity. For one tilting direction (positive voltage in Figs. 2 and 5), the force required to move the ions through the pore is smaller than in the other direction (negative voltage in Figs. 2 and 5) when the ions are “trapped” inside the pore.<sup>30</sup> Even if the voltage applied across the membrane fluctuates with a zero mean, a net flow of ions is observed. When there is a concentration gradient across the membrane, the tooth is tilted additionally by the Nernst potential. Therefore, we have to apply a higher amplitude external field to make the ions move against the concentration gradient. This mechanism of producing a “force-free”<sup>31</sup> net flow in the absence of macroscopic forces is called the ratchet mechanism with a fluctuating force or a rocking ratchet.<sup>30</sup>

Figure 6 shows examples of trajectories of ions passing through the conical pore, starting from two entrances of the cone for the same parameters as in Fig. 4(b). These results confirm the preferential movement of ions in the direction toward the wide opening of the pore. In Ref. 40 we obtained very similar results for another set of parameters:  $r_0 = 1$  nm, different phases of the oscillating field instead of different initial velocities (equivalent to low values of  $v_0$ ),  $1/\lambda = 300$  nm,  $\gamma/m = 0.005$  s<sup>-1</sup>, and the potential  $V(z)$  calculated from the charges distributed along the walls of a two-dimensional cone. This agreement suggests that the model

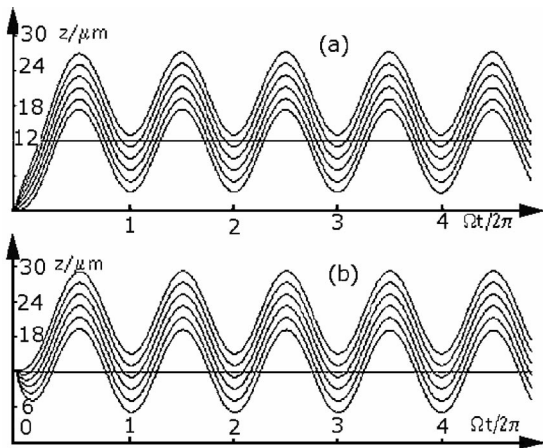


Fig. 6. Trajectories of a positive ion starting to cross the pore close to the (a) narrow and (b) the wide opening of the pore, calculated from Eq. (8) with the same parameters as Fig. 4. The horizontal line at  $z = 12$   $\mu\text{m}$  marks the wide exit from the pore.

predicts the qualitative behavior of the system for a wide range of parameters. The most important quality is the existence of the asymmetric profile of the potential, which in turn determines the behavior of the system.

The attentive reader may notice at this point that the trajectories shown in Fig. 6 oscillate near the wide exit/entrance of the pore, whereas the trajectories calculated in Ref. 40 do not. This difference is in part the result of different time scales and is due in part to much higher friction and initial velocities in the present calculations. (If the trajectories from Fig. 6 were sufficiently stretched to show the first passage when the ions traveled the whole length of the pore for the first time the oscillations would not be visible.)

Next we discuss how the physical properties of the electrolyte constrained in a narrow channel are different from the bulk solution. We begin with the screening length  $L_D = 1/\lambda$ , which in the bulk is of the order of 1 nm. Experimental data show that the pore is cation-selective, that is, at least in the narrow part of the pore, the anions are depleted. At the very tip there are probably no mobile anions (in our case  $\text{Cl}^-$ ) due to the strong repulsion from negative charges on the pore walls. There is just no place for them, which implies that there is no screening.

There is no direct way to determine the value of the friction coefficient inside the pore. The relation between the electric field induced by charges inside the pore and the applied oscillating electric field is not well understood. The amplitude  $A$  of the oscillating applied potential difference is known. The density  $\rho$  of the charges on the pore walls is about one elementary charge per square nanometer, which gives us a basis for determining the internal field. However,  $A$  is measured with respect to some arbitrary reference potential  $V_0$  (we measure the potential difference), whereas the potential resulting from the charge  $\rho$  can be calculated with respect to another zero-potential corresponding to zero charge. Measurements of the value of  $V_0$  at zero charge are not straightforward. The mass of an ion in a solution is not well defined either. In an electrolytic solution, the ions are hydrated (that is, they move together with a few water molecules; how many, we do not really know), which increases the mass to as much as 100  $\mu$ .

All these considerations and uncertainties point out that the design of synthetic systems with known geometry and chemical structure can be helpful for understanding phenomena occurring on a nanometer scale. It is important to build theoretical models with physical parameters, which subsequently can be found by fitting the experimental data.

**Problem 3:** Write a program that calculates the potential  $V(z)$  and force  $F(z)$ , and solves Eq. (8). Find the ion’s trajectories for different sets of parameters.

**Project 1:** Find expressions for the potential  $V(z, r)$  inside the entire cone, not only along the cone axis [see Eq. (7)]. (To avoid infinities, remember that ions are not point-like, but have finite diameters). Next, write an equation for the three-dimensional motion of an ion and solve it numerically.

## VI. DESCRIPTION OF ION TRANSPORT BY SMOLUCHOWSKI EQUATION

The simple single-ion-motion model presented in Sec. V explains the qualitative behavior of asymmetric nanopores. However, it is not suited for calculating the ion current, which is the main observable of the properties of the nanopore. We note that a ion current of 1 nA corresponds to  $\sim 10^9$

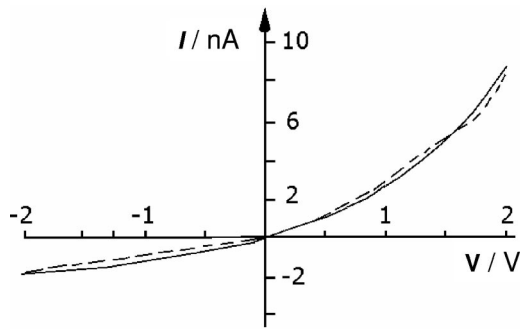


Fig. 7. Dependence of  $I$  on the voltage  $V$ , both measured (dashed line) and calculated from Eq. (11) (full line) for equal concentrations on both sides of the pore ( $c_0 = c_L$ ). The parameters  $D$ ,  $U$ , and  $\beta$  were fitted to experimental data; the intrinsic parameters are the same as in Figs. 4(b) and 6. These results show the rectifying properties of the nanopore.

ions passing the pore in 1 s. One disadvantage of the single-ion approach is the difficulty of introducing interactions of the ion with other ions in the solution and with water—friction is the only parameter describing these effects. Moreover, this model does not take into account either thermal fluctuations or fluctuations due to the small size of the pore, which significantly influence the ionic movement. The fluctuations could be introduced by adding the noise component directly into Eq. (8), but the resulting stochastic differential equation is very difficult to solve numerically. One way to overcome these difficulties incorporates a hydrodynamic approach through the generalized diffusion (electro-diffusion, Smoluchowski) equation:<sup>51</sup>

$$\frac{\partial c(z,t)}{\partial t} = -\frac{\partial}{\partial z} J(z,t), \quad (9)$$

$$J(z,t) = -D \frac{\partial c(z,t)}{\partial z} + \mu F_{\text{tot}}(z) c(z,t), \quad (10a)$$

$$F_{\text{tot}} = -\frac{\partial V_{\text{tot}}(z)}{\partial z}, \quad (10b)$$

$$V_{\text{tot}} = W(z) + V(z), \quad (10c)$$

where  $\mu$  is the ion mobility,  $D$  is the diffusion constant,  $c$  is the concentration,  $J(z,t)$  is the flow (current density) of the ions, and  $W(z)$  is the external electric potential.

The following simplifications can be applied in our case. In the stationary state,  $c$  and  $J$  do not depend on time (remember that the external field changes adiabatically). In addition, by mass (charge) conservation, in one-dimension  $J$  does not depend on  $z$ . Equation (10) then becomes a simple nonuniform first-order ordinary differential equation. If we assume that the internal potential outside the pore is equal to zero, and solve Eq. (10) for  $z=L$  with the initial condition at  $z=0$ , we obtain:

$$J = D \frac{c_0 e^{\beta W(0)} - c_L e^{\beta W(L)}}{\int_0^L dz e^{\beta[W(z)+V(z)]}}, \quad (11)$$

where  $\beta = \mu/D$ . If we substitute  $V(z)$  from Eq. (7), and let  $W(z) = Uz/L$  with  $U$  the external voltage, it is easy to calculate the current density  $J$ , and therefore the current  $I$  together with the net current  $\langle I \rangle$ . A comparison of the measured  $I$  and the value calculated from Eq. (11) is shown in Fig. 7.

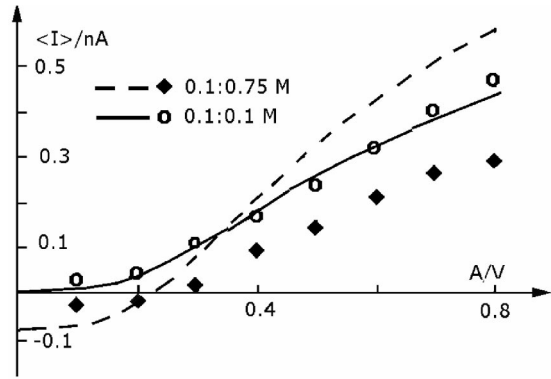


Fig. 8. Comparison of experimental data for the net current through a single conical pore for equal (circles) and unequal (diamonds) concentrations on both sides of the membrane, using Eq. (11). The following parameters were used:  $D_{\text{eff}}=2.5$ ,  $A_{\text{eff}}=35$ ,  $\beta_{\text{eff}}=7$ ,  $\rho_{\text{eff}}=0.1$ , which for  $A=0.8$  V and  $I=0.5$  nA (symmetric electrolyte conditions) correspond to the physical quantities:  $D=4 \times 10^9$  nm<sup>2</sup>/s ( $D_{\text{bulk}}=2 \times 10^9$  nm<sup>2</sup>/s),  $\beta=306$  V<sup>-1</sup>,  $\rho=5.2 \times 10^{-4}$  V/nm.

Figure 8 shows the net current  $\langle I \rangle$  determined from the experimental data [Fig. 3(b)] by averaging the current over the period of the ac signal, together with the fit obtained by Eq. (11). These results show that it is possible to fit the parameters of the model only to some of the experimental data. The model reproduces very well the experiments for symmetric electrolyte conditions. However, if we use the same parameters for the system with a concentration gradient, we obtain an incorrect prediction for the current (dashed line and diamonds in Fig. 8). On the other hand, it is possible to find another set of parameters that reproduce well the data for asymmetric electrolyte conditions, but that work badly for  $c_0 = c_L = 0.1$  M. However, Eq. (11) incorrectly reproduces the dependence of the rectification and pumping effect on the diameter of the narrow aperture. These results imply that we should be careful with conclusions drawn from simplified models.

*Problem 5:* Discuss how the assumption of the adiabatic character of the ion current changes when the conical pore is described by the three-dimensional model. How will Eq. (11) change?

*Problem 6:* Write a program to solve Eq. (11) and calculate the current–voltage characteristic together with the net current  $\langle I \rangle$  for  $c_0 \neq c_L$ .

*Problem 7:* Consider the case  $V(z)=0$ . Calculate analytically the ion current from Eq. (11) for  $c_0 \neq c_L$ ,  $U=0$ , and  $c_0 = c_L$ ,  $U \neq 0$ . Compare the results with Fick's and Ohm's laws.

The use of one-dimensional models, both in Sec. V (cf. Project 1), and especially in the diffusion approach, requires some justification. The one-dimensional (1D) description in restricted geometries can be understood as a three-dimensional (3D) geometry averaged over directions perpendicular to the pore's  $z$  axis. Such an average is legitimate only under several additional conditions that are too specific to be discussed here (see, for example, Refs. 51–53). More important, however, is to point out the price of such a 1D projection. The reduction of a three-dimensional to a one-dimensional model leads to the interpretation of physical parameters as effective ones. For example, the Debye screening length in a 0.1 M 1:1 electrolytic solution is about 1 nm. The average of the real, 3D screened internal electrostatic poten-

tial  $V(z, r; \lambda)$  (from Project 1 in Sec. V) results in the effective potential  $V_{\text{eff}}(z; \lambda_{\text{eff}})$  with the effective screening length  $1/\lambda_{\text{eff}}$ . Both analytical (very rough) estimates, and numerical (very lengthy) computations imply that the effective screening length is at least two orders of magnitude larger than the screening length in three dimensions (this is one of the reasons why here and in Ref. 40 we used  $L_D \gg 1$  nm). The same problems appear on an even greater scale in the description of transport through biological channels, that is, nanopores built of proteins that are even narrower and shorter than those considered here. Interested readers will find discussions in Refs. 52 and 53.

*Project 2:* Use the potential  $V(z, r; \lambda)$  from Project 1 to estimate analytically and numerically the effective screening length. Hint: average  $V(z, r; \lambda)$  over  $r$ , both directly and using the procedure given in Ref. 51, and compare the results with  $V_{\text{eff}}(z; \lambda_{\text{eff}})$  calculated from Eq. (7). To simplify the task, you may use a two-dimensional description instead of a three-dimensional one (especially in numerical computations), a cylindrical ( $r_0 = r_L$ ) instead of a conical geometry, and a much shorter pore (a length of about 50 nm will suffice). In analytical estimations, look for the greatest contributions to the relevant integrals [the smaller  $R(z, z', r)$  is in analogs of Eq. (7), the greater the integral].

The reasons for the unsatisfactory results of the generalized diffusion model lie not only in the several approximations that we have above. The main question is whether this type of model is applicable to nanometer-sized pores. Diffusional (hydrodynamic) descriptions involve quantities such as the diffusion coefficient, concentration, and current, that is, average (macroscopic) quantities usually associated with many particles. On the other hand, the narrow part of the pore—a few nanometers in diameter—is of the order of a few ion diameters (the  $K^+$  diameter in a crystal is about 0.27 nm, that of a hydrated  $K^+$  is about 0.7 nm). It is known that in very narrow channels with charged walls the ions move in single file (cf. Refs. 19 and 54). This motion makes the application of a continuous description questionable.

A correct three-dimensional theory, taking into account as much geometrical and electrostatic details as possible, together with further measurements in narrow pores of various geometries and various distributions of internal fields, are needed to settle this intriguing problem. We are currently working on these issues both experimentally and theoretically. Further studies should also answer the question if and how the pore differentiates between various cations. Systematic studies with monovalent cations from lithium to cesium as well as polyvalent cations will give us information on the influence of the internal pore potential on the cation's movement. We will also check if the potential of the pore changes when various cations pass through the pore.

## VII. CONCLUSIONS

We have discussed the track etching technique for structuring materials on the nanometer scale. The preparation of single asymmetric nanopores in polymer foils was described together with the methods to study their transport properties. We demonstrated that when the dimensions of the pore are on the order of nanometers, the pore changes its transport characteristics. A conically shaped, charged nanopore is cation selective and acts as a diode with a preferential direction for the cation flow from the narrow entrance toward the wide

opening of the pore. Moreover, the asymmetric nanopore transports ions against their concentration gradient when a fluctuating electric force is applied across the membrane. An intuitive qualitative model of the ionic rectification and pumping was based on the ratchet mechanism with a fluctuating force. We also discussed the applicability of the Smoluchowski equation to the quantitative description of ion transport through nanopores.

The suggested calculations and numerical simulations (the tasks marked as projects are more challenging) will help physics students understand phenomena occurring on a nanoscale.

## ACKNOWLEDGMENTS

Z.S. was supported by the Alexander von Humboldt Foundation. The hospitality of the Department of Materials Research of the Gesellschaft für Schwerionenforschung in Darmstadt is greatly appreciated. The authors would like to thank C. Trautmann, E. M. Toimil-Molares, I. Kosińska, P. Apel, D. D. Dobrev, Y. E. Korchev, R. Neumann, and R. Spohr for stimulating discussions.

<sup>a</sup>Electronic mail: z.siw@gsi.de

<sup>1</sup>R. Feynman, "Engineering and science," *Caltech* **23**, 22–36 (1960).

<sup>2</sup>Special volume of *Science* **254**, 1300–1342 (1991).

<sup>3</sup>D. Appell, "Wired for success," *Nature (London)* **419**, 553–555 (2002).

<sup>4</sup>E. Toimil-Molares, V. Buschmann, D. Dobrev, R. Neumann, R. Scholz, I. U. Schuchert, and J. Vetter, "Single-crystalline copper nanowires produced by electrochemical deposition in polymeric ion track membranes," *Adv. Mater. (Weinheim, Ger.)* **13**, 62–65 (2001).

<sup>5</sup>E. Toimil-Molares, J. Brotz, V. Buschmann, D. Dobrev, R. Neumann, R. Scholz, I. U. Schuchert, C. Trautmann, and J. Vetter, "Etched heavy ion tracks in polycarbonate as template for copper nanowires," *Nucl. Instrum. Methods Phys. Res. B* **185**, 192–197 (2001).

<sup>6</sup>J. C. Hulthen and C. R. Martin, "A general template-based method for the preparation of nanomaterials," *J. Mater. Res.* **7**, 1075–1087 (1997).

<sup>7</sup>K. B. Jirage, J. C. Hulthen, and C. R. Martin, "Nanotubule-based molecular-filtration membranes," *Science* **278**, 655–658 (1997).

<sup>8</sup>M. S. Gudiksen and C. M. Lieber, "Diameter-selective synthesis of semiconductor nanowires," *J. Am. Chem. Soc.* **122**, 8801–8802 (2000).

<sup>9</sup>D. R. Stewart, D. Sprinzak, C. M. Marcus, C. I. Duruöz, and J. S. Harris, Jr., "Correlations between ground and excited state spectra of a quantum dot," *Science* **278**, 1784–1788 (1997).

<sup>10</sup>H. Linke, T. E. Humphrey, A. Löfgren, A. O. Sushkov, R. Newbury, R. P. Taylor, and P. Omling, "Experimental tunneling ratchets," *Science* **286**, 2314–2317 (1999).

<sup>11</sup>M. S. Gudiksen, L. J. Lauhon, J. Wang, D. C. Smith, and C. M. Lieber, "Growth of nanowire superlattice structures for nanoscale photonics and electronics," *Nature (London)* **415**, 617–620 (2002).

<sup>12</sup>B. Hille, *Ionic Channels of Excitable Membranes* (Sinauer, Sunderland, MA, 1992), 2nd ed.

<sup>13</sup>Y. Zhou, J. H. Morais-Cabral, A. Kaufmann, and R. MacKinnon, "Energetic organization of ion conduction rate by the  $K^+$  selectivity filter," *Nature (London)* **414**, 37–42 (2001).

<sup>14</sup>Y. Jiang, A. Lee, J. Chen, M. Cadene, B. T. Chait, and R. MacKinnon, "The open pore conformation of potassium channels," *Nature (London)* **417**, 523–526 (2002).

<sup>15</sup>*Cell Physiology*, edited by N. Sperelakis (Academic, San Diego, CA, 1998).

<sup>16</sup>E. Neher and B. Sakmann, "Single-channel current recorded from membrane of denervated frog muscle fibers," *Nature (London)* **260**, 799–802 (1976).

<sup>17</sup>E. Gorczynska, P. L. Huddle, B. A. Miller, I. R. Mellor, H. Vais, R. L. Ramsey, and P. N. R. Usherwood, "Potassium channels of adult locust *Schistocerca gregaria* muscle," *Pfluegers Arch.* **432**, 597–606 (1996).

<sup>18</sup>D. A. Doyle, J. M. Cabral, R. A. Pfuetzner, A. Kuo, J. M. Gulbis, S. L. Cohen, B. T. Chait, and R. MacKinnon, "The structure of the potassium channel: Molecular basis of  $K^+$  conduction and selectivity," *Science* **280**, 69–77 (1998).

<sup>19</sup>Y. Jiang, A. Lee, J. Chen, M. Cadene, B. T. Chait, and R. MacKinnon,

- "Crystal structure and mechanism of a calcium-gated potassium channel," *Nature (London)* **417**, 515–522 (2002).
- <sup>20</sup>G. Yellen, "The voltage-gated potassium channels and their relatives," *Nature (London)* **419**, 35–42 (2002).
- <sup>21</sup>Z. Siwy and A. Fulinski, "Origins of  $1/f^\alpha$  noise in membrane channels currents," *Phys. Rev. Lett.* **89**, 158101-1–158101-4 (2002).
- <sup>22</sup>J. J. Kasianowicz, E. Brandin, D. Branton, and D. W. Deamer, "Characterization of individual polynucleotide molecules using a membrane channel," *Proc. Natl. Acad. Sci. U.S.A.* **93**, 13770–13773 (1996).
- <sup>23</sup>C. A. Pasternak, C. L. Bashford, Y. E. Korchev, T. K. Rostovtseva, and A. A. Lev, "Modulation of surface flow by divalent cations and protons," *Colloids Surf., A* **77**, 119–124 (1993).
- <sup>24</sup>Y. E. Korchev, C. L. Bashford, G. M. Alder, P. Y. Apel, D. T. Edmonds, A. A. Lev, K. Nandi, A. V. Zima, and C. A. Pasternak, "A novel explanation for fluctuations of ion current through narrow pores," *FASEB J.* **11**, 600–608 (1997).
- <sup>25</sup>Z. Siwy, Y. Gu, H. A. Spohr, D. Baur, A. Wolf-Reber, R. Spohr, P. Apel, and Y. E. Korchev, "Rectification and voltage gating of ion currents in a nanofabricated pore," *Europhys. Lett.* **60**, 349–355 (2002).
- <sup>26</sup>Z. Siwy, P. Apel, D. Baur, D. Dobrev, Y. E. Korchev, R. Neumann, R. Spohr, C. Trautmann, and K. Voss, "Preparation of synthetic nanopores with transport properties analogous to biological channels," *Surf. Sci.* **532–535**, 1061–1066 (2003).
- <sup>27</sup>Z. Siwy, D. D. Dobrev, R. Neumann, C. Trautmann, and K. Voss, "Electro-responsive asymmetric nanopores in polyimide with stable ion current signal," *Appl. Phys. A: Mater. Sci. Process.* **76**, 781–785 (2003).
- <sup>28</sup>R. D. Astumian, "Making molecules into motors," *Sci. Am.* **285** (7), 56–64 (2001).
- <sup>29</sup>C. Marquet, A. Buguin, L. Talini, and R. Silberzan, "Rectified motion of colloids in asymmetrically structured channels," *Phys. Rev. Lett.* **88**, 168301-1–168301-4 (2002).
- <sup>30</sup>R. D. Astumian, "Thermodynamics and kinetic of a Brownian motor," *Science* **276**, 917–922 (1997).
- <sup>31</sup>P. Hänggi and R. Bartussek, "Brownian rectifiers: How to convert Brownian motion into directed transport," in *Nonlinear Physics of Complex Systems*, edited by J. Parisi, S. C. Müller, and W. Zimmermann (Springer, Berlin, 1997), Vol. 476, pp. 294–308.
- <sup>32</sup>R. D. Astumian and P. Hänggi, "Brownian Motors," *Phys. Today* **55** (11), 33–39 (2002).
- <sup>33</sup>R. D. Astumian and I. Derenyi, "Fluctuation driven transport and models of molecular motors and pumps," *Eur. Biophys. J.* **27**, 474–489 (1998).
- <sup>34</sup>R. L. Fleischer, P. B. Price, and R. M. Walker, *Nuclear Tracks in Solids. Principles and Applications* (University of California Press, Berkeley, 1975).
- <sup>35</sup>R. Spohr, *Ion Tracks and Microtechnology. Principles and Applications* (Vieweg, Braunschweig, 1990).
- <sup>36</sup>R. Spohr, "Methods and device to generate a predetermined number of ion tracks," German Patent DE 2951376 C2 (1983); United States Patent No. 4369370 (1983).
- <sup>37</sup>The polymer film of polyethylene terephthalate, Hostaphan, RN12 produced by Hoechst was used in the experiments.
- <sup>38</sup>C. R. Martin, M. Nishizawa, K. Jirage, M. Kang, and S. B. Lee, "Controlling ion-transport selectivity in gold nanotubule membranes," *Adv. Mater. (Weinheim, Ger.)* **13**, 1351–1362 (2001).
- <sup>39</sup>G. Guillot and F. Rondelez, "Characteristics of submicron pores obtained by chemical etching of nuclear tracks in polycarbonate films," *J. Appl. Phys.* **5**, 7155–7164 (1981).
- <sup>40</sup>Z. Siwy and A. Fulinski, "Fabrication of a synthetic nanopore ion-pump," *Phys. Rev. Lett.* **89**, 198103-1–198103-4 (2002).
- <sup>41</sup>E. H. Serpersu and T. Y. Tsong, "Activation of electrogenic Rb<sup>+</sup> transport of (Na,K)-ATPase by an electric field," *J. Biol. Chem.* **259**, 1755–1762 (1984).
- <sup>42</sup>T. Y. Tsong, "Electroconformational coupling: A fundamental process of biomolecular electronics for signal transduction," in *Molecular Electronics. Biosensors and Biocomputers*, edited by F. T. Hong (Plenum, New York, 1989), pp. 83–95.
- <sup>43</sup>D.-S. Liu, R. D. Astumian, and T. Y. Tsong, "Stimulation of the Na<sup>+</sup> and K<sup>+</sup> pump of NaK ATPase by ac electric field," *J. Biol. Chem.* **265**, 7260–7267 (1990).
- <sup>44</sup>T. D. Xie, P. Marszalek, Yi-der Chen, and T. Y. Tsong, "Recognition and processing of randomly fluctuating electric signals by Na,K-ATPase," *Biophys. J.* **67**, 1247–1251 (1994).
- <sup>45</sup>T. D. Xie, Yi-der Chen, P. Marszalek, and T. Y. Tsong, "Fluctuation-driven directional flow in biochemical cycle: Further study of electric activation of Na, K pumps," *Biophys. J.* **72**, 2496–2502 (1997).
- <sup>46</sup>A. Fulinski, "Driven chemical kinetics: Optimization of catalytic action of membrane proteins by rectangular alternating electric field," *J. Chem. Phys.* **96**, 3549–3558 (1992).
- <sup>47</sup>A. Fulinski, "Noise-stimulated active transport in biological cell membranes," *Phys. Lett. A* **193**, 267–273 (1994).
- <sup>48</sup>A. Fulinski, "Active transport in biological membranes and stochastic resonances," *Phys. Rev. Lett.* **79**, 4926–4929 (1997).
- <sup>49</sup>A. Fulinski, "Barrier fluctuations and stochastic resonance in membrane transport," *Chaos* **8**, 549–556 (1998).
- <sup>50</sup>A. Fulinski and P. F. Góra, "Constructive role of noise in signal transmissions by biomembrane proteins," *Phys. Rev. E* **64**, 011905-1–011905-11 (2001).
- <sup>51</sup>R. Zwanzig, "Diffusion past an entropy barrier," *J. Phys. Chem.* **96**, 3926–3930 (1992).
- <sup>52</sup>W. Nonner, D. P. Chen, and B. Eisenberg, "Progress and prospects in permeation," *J. Gen. Physiol.* **113**, 773–782 (1999).
- <sup>53</sup>D. G. Levitt, "Modeling of ion channels," *J. Gen. Physiol.* **113**, 789–794 (1999).
- <sup>54</sup>S. Berneche and B. Roux, "Energetics of ion conduction through the K<sup>+</sup> channel," *Nature (London)* **414**, 73–76 (2001).